The evolution of relaxation modes during isothermal annealing and its influence on properties of Fe-based metallic glass

Nana He[a,b], Lijian Song[a,b], Wei Xu[a,b], Juntao Huo[a,b,*], Jun-Qiang Wang[a,b,*], Run-Wei Li[a,b]

[a] CAS Key Laboratory of Magnetic Materials and Devices, Zhejiang Province Key Laboratory of Magnetic Materials and Application Technology, Ningbo Institute of Materials Technology and Engineering, Chinese Academy of Sciences, Ningbo 315201, China
[b] Center of Materials Science and Optoelectronics Engineering, University of Chinese Academy of Sciences, Beijing 100049, China

ARTICLE INFO

ABSTRACT

Isothermal annealing can enhance the soft magnetic properties of Fe-based metallic glasses, but usually causes brittleness. In this work, we studied the relaxation kinetics of Fe-based metallic glasses below glass transition temperature and the evolution of soft magnetic properties and plasticity. We found that the metallic glass first experiences secondary (β) relaxation and then transforms into primary (α) relaxation upon isothermal annealing. The magnetic properties are enhanced predominantly during β relaxation stage but don't change very much during α relaxation stage. The plasticity doesn't change very much during β relaxation stage but gets deteriorated during α relaxation stage. The structural origin of the changes is also studied. These results prove that it is probable to achieve metallic glasses with both excellent soft magnetic properties and excellent mechanical properties by controlling the relaxation process, which may provide a universal protocol for enhancing the functional performance of soft magnetic metallic glasses.

1. Introduction

Soft magnetic Fe-based metallic glasses exhibit excellent energy-saving characters owing to the combination of low coercivity, high permeability and high electrical resistivity [1–4]. However, the magnetic properties of as-cooled metallic glasses are not soft enough, because severe internal stress is frozen during the shear spinning production process. The magnetic anisotropy that arises from the magnetoelastic coupling effect hinders the movement of magnetic domains. To improve the soft magnetic properties, it is usually annealed below the glass transition temperature to release the internal stress. However, annealing usually causes embrittlement, which makes the electronics fragile and may cause electric short circuit [5–7].

A lot of efforts have been devoted to avoiding the annealing-embrittlement, e.g. exploring new materials and searching for the intrinsic parameters to control it [8,9]. Kumar, et al. proposed using the fictive temperature to characterize the ductile-to-brittle transition [9]. The critical fictive temperature depends on sample size that suggests it may not be an ideal parameter for evaluation. Isothermal annealing has been regarded as a single relaxation process which can be fitted using an extended exponential equation [10–13]. However, recent experimental results reveal that metallic glasses experience multiple relaxation modes during isothermal annealing with/without external stress [14–18]. Under stress, the Zr-, CuZr-, La-based metallic glasses exhibit two-step relaxations, one is stress-driven fast relaxation and the other is thermal activated slow process [15,16]. Without stress, experiments confirm that Au-based metallic glasses first experience β relaxation and then transform to α relaxation during isothermal annealing or multiple-step relaxations during isothermal annealing [14,18]. It is intriguing to testify whether Fe-based metallic glasses also experience various relaxation modes during isothermal annealing, and the roles of various relaxations in modifying the properties.

In this letter, we studied the evolution of relaxation kinetics of a soft magnetic Fe-based metallic glass using differential scanning calorimetry (DSC). The influence of various relaxation modes, e.g. β relaxation and α relaxation, on magnetic and mechanical properties is studied. The microstructural origin for these evolutions is also revealed.

2. Experimental

The master alloy of $Fe_{77}Si_{2.71}B_{14.88}P_{4.06}C_{1.35}$ (at.%) were prepared by induction melting the mixtures of Fe (99.99 wt%), Si (99.999 wt%), B (99.99 wt%), Fe−P alloy (99.9 wt%) and Fe−C alloy (99.9 wt%) in an argon atmosphere. The master alloy was re-melted and subsequently

* Corresponding authors at: CAS Key Laboratory of Magnetic Materials and Devices, Zhejiang Province Key Laboratory of Magnetic Materials and Application Technology, Ningbo Institute of Materials Technology and Engineering, Chinese Academy of Sciences, Ningbo 315201, China.
E-mail addresses: huojuntao@nimte.ac.cn (J. Huo), jqwang@nimte.ac.cn (J.-Q. Wang).

injected onto a spinning copper roller (tangent velocity of about 40 m/s) to obtain metallic glass ribbons. The amorphous structure is verified by X-ray diffraction with Cu-K_α radiation. The thermal properties were studied using a differential scanning calorimeter (DSC, Netzsch 404C) in standard platinum crucibles under a constant flow of high-purity argon gas (100 ml/min). Ribbons for magnetic property measurements were annealed for different time in a furnace under a high vacuum of about 10^{-3} Pa. Coercivity (H_C) was measured with a *dc B−H* loop tracer under a field of 800 A/m. Effective permeability (μ_e at 1 kHz) was measured with an impedance analyzer with a field of 1 A/m. To eliminate the influence of demagnetizing factors on soft-magnetic properties, the length of the ribbons for DC B−H loop tracer and impedance analyze measurement is 50 mm which is much larger than the width and thickness. The viscoelastic heterogeneity of the metallic glass ribbon was investigated using amplitude-modulation atomic force microscope (AM-AFM), produced by Bruker Company. The probe tip is silicon with a force constant of about 40 N/m and the curvature radius of about 2 nm. The bending plasticity was measured by a home-made bending tester, which has the displacement rate of 1 mm/min. The fracture radius (r_f) can be recorded when the sample that locates between upper and lower magnetics substrates was broken.

3. Results and discussion

Fig. 1(a) shows the XRD pattern of the as-quenched
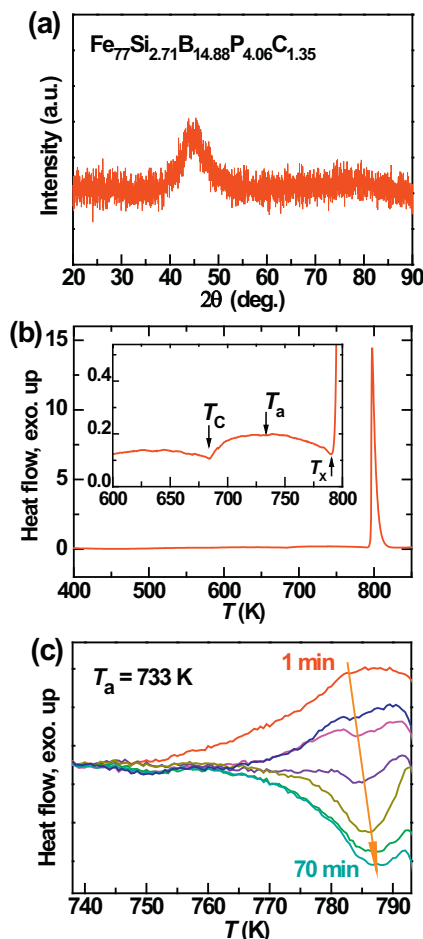
Fig. 1. (a) The XRD pattern of the as-spun $Fe_{77}Si_{2.71}B_{14.88}P_{4.06}C_{1.35}$ ribbon. (b) The DSC trace of $Fe_{77}Si_{2.71}B_{14.88}P_{4.06}C_{1.35}$ metallic glass at heating rate of 40 K/min. The inset is the magnified part close to Curie temperature T_c and crystallization temperature T_x. (b) Change of heat flows after being annealed at 733 K for various times.
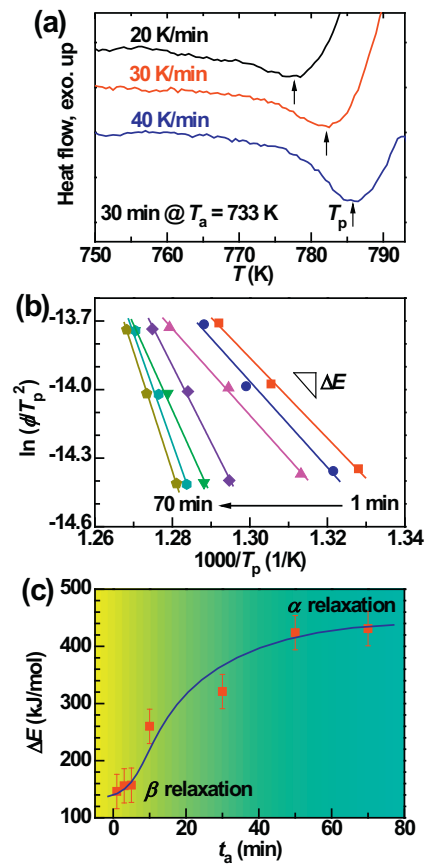
Fig. 2. (a) The heat flows at different heating rates for the sample preannealed at 733 K for 30 min. (b) The Kissinger plot of the relaxation peak for samples preannealed at 733 K for various time. (c) The evolution of relaxation barrier along with annealing time t_a. The yellow background zone represents β relaxation stage and the cyan background represents α relaxation stage.

$Fe_{77}Si_{2.71}B_{14.88}P_{4.06}C_{1.35}$ alloy ribbon. The pattern shows broad diffraction maxima and no sharp Bragg peaks from crystalline phases, indicating the fully amorphous microstructure of the samples. Fig. 1(b) shows the DSC trace of the as-spun ribbon. A large exothermic crystallization peak is observed, which confirms the amorphous nature. The onset temperature (T_x) of crystallization is about 793 K, the magnetic transition temperature (T_C) is determined to be about 696.5 K. An intermediate temperature ($T_a = 733$ K) between T_x and T_C is selected to study the isothermal relaxation kinetics. When being annealed at 733 K, the heat flow overshoot increases along with the annealing time ($t_a = 1$–70 min). To better illustrate the evolvement of relaxation peak, the change of heat flows after annealing are shown in Fig. 1(c), which are obtained by subtracting the DSC trace of initial sample from the annealed samples. The relaxation peak in heat flow changes from an exothermic-like behavior to endothermic-like characters, which confirms the decrease of enthalpy upon annealing. The relaxation peak (T_p) shifts to higher temperature along with the increase of annealing time.

To study the kinetics of the relaxation progress, the relaxation peak is measured at various heating rates, as shown in Fig. 2(a). The activation energy of relaxation (ΔE) is determined by Kissinger's equation [19,20].

$$\ln\left(\frac{\phi}{T_p^2}\right) = \frac{\Delta E}{R\,T_p} + C$$

where ϕ is the heating rate, R the gas constant. As shown in Fig. 2(b), the slope of the linear fitting result is determined to be $-\Delta E/R$. Fig. 2(c) shows the evolution of activation energy along with annealing time. It
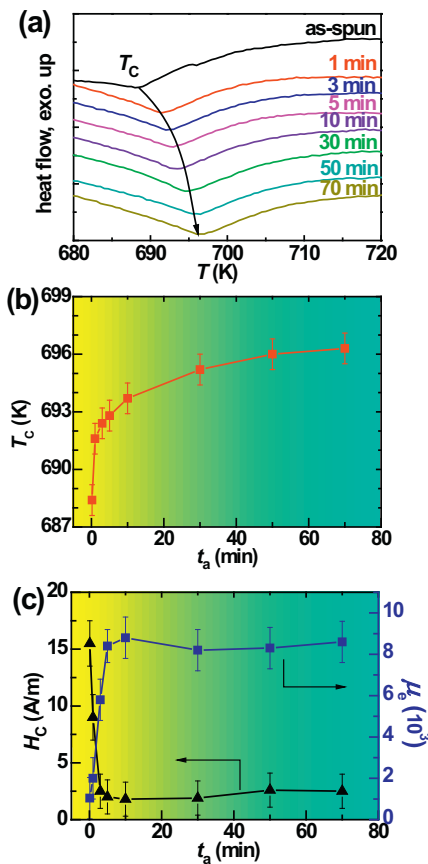
Fig. 3. (a) The DSC traces close to the magnetic phase transition range for samples preannealed at 733 K for various time, with a curve showing the change of T_c. (b) The evolution of T_c along with t_a. (c) The evolution of H_c (left axis) and μ_e (right axis) along with annealing time t_a.

is about 150 kJ/mol when the annealing time is less than 10 min, which is about $24RT_g$ almost equal to the activation energy of β relaxation [21]. When the annealing time increases, the activation energy increases to about 430 kJ/mol, which is close to the activation energy of α relaxation (with a fragility of about 30 [22]). Such a transition from β relaxation to α relaxation is similar to that observed in Au-based metallic glasses [14]. It is intriguing to study how the different relaxation process influences the properties of Fe-based metallic glasses.

The Curie temperature (T_C) represents the temperature where ferromagnetic state transforms to paramagnetic states. Such a phase transition can be measured by DSC, as shown in Fig. 3(a). It shifts to higher temperatures along with the increase of annealing time, which denotes the magnetic coupling interaction becomes stronger. As shown in Fig. 3(b), T_C increases fast for short-time annealing that corresponds to the β relaxation stage, while it does not change very much during α relaxation stage. The evolution of coercivity (H_C) and effective permeability (μ_e) are also studied, as shown in Fig. 3(c). H_C decreases and μ_e increases sharply during the β relaxation stage, while they do not change very much during α relaxation stage.

Embrittlement caused by annealing has been a huge challenge for the application of Fe-based metallic glasses. For practical application, the Fe-based metallic glasses are bended into a circle or square, so their bending plasticity is very important. The bending plasticity is studied using a home-made bending test machine, as schematically illustrated in Fig. 4(a), to reveal the effect of different relaxation modes on the plastic deformability. The metallic glass ribbon is held between two clamps. The loading rate of the clamp is 1 mm/min. Once the ribbon breaks, the sensor will record the distance between two clamps which is two times of the fracture radius (r_f). A smaller fracture radius represents
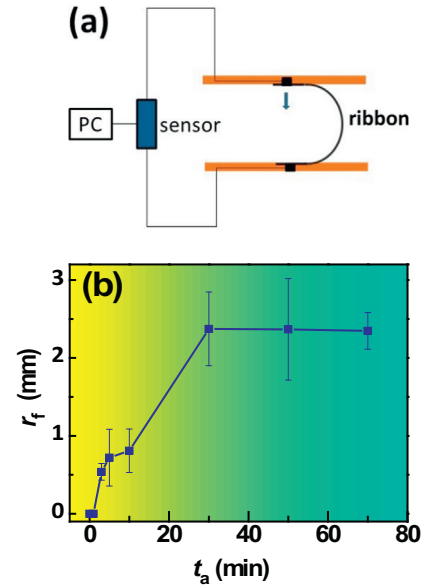
Fig. 4. (a) Schematic illustration of the apparatus for bending plasticity test. The displacement rate is 1 mm/min. The fracture radius (r_f) is detected automatically. (b) The evolution of fracture radius along with annealing time t_a.

better plasticity. As shown in Fig. 4(b), the as-pun ribbon can be folded by 180°. During the β relaxation stage, the fracture radius remains smaller than 1 mm that is ductile enough for applications. After reaching the α relaxation stage, the ribbon becomes brittle with a fracture radius of about 2 mm.

To study the correlation between the structure and properties, the microstructure is investigated using AM-AFM. Fig. 5 shows the AFM images of samples annealed at $T_a = 733$ K for different annealing time ($t_a = 1$–70 min). All the samples exhibit typical nanoscale heterogeneity that is observed in other metallic glasses [23–26]. Along with the increase of annealing time, the viscoelastic dissipation energy (E_{dis}) decreases that suggest the annihilation of free volumes. This is consistent with previous results that observed in Zr-based metallic glasses [26]. In the β relaxation stage, it is interesting that the E_{dis} decreases sharply but remains a large level. In α relaxation stage, the E_{dis} becomes as small as 40 eV. According to viscoelastic deformation model [27,28], the large E_{dis} denotes a high concentration of free volume that benefits the plastic deformation. The recent work reports that there is a correlation between the viscoelastic heterogeneity and the motion of domain walls [29]. Thus, the decrease of E_{dis} during β relaxation allows domain walls move easily under an external magnetic field and enhances the macro magnetic properties.

This work presents evidence that β relaxation plays an important role in modulating the functional properties of metallic glasses. Such an intrinsic correlation between β relaxation and magnetic properties may advise answers for some important scientific and technical questions. For instance, it has been long-lasting questions why annealing at too low temperature or too high temperature will not change T_C very much and why the T_C of some metallic glasses are not sensitive to annealing [30]. On the other hand, the small E_{dis} when reaching the α relaxation stage suggests that the embrittlement may origin from the annihilation of dynamically viscous zones, e.g. flow units or shear transformation zones. These results provide a general strategy to achieve metallic glasses with both enhanced soft magnetic properties and good mechanical properties by controlling the relaxation process.

4. Conclusions

In summary, we found that the Fe-based metallic glass experiences two steps during isothermal annealing, i.e. first β relaxation and then α
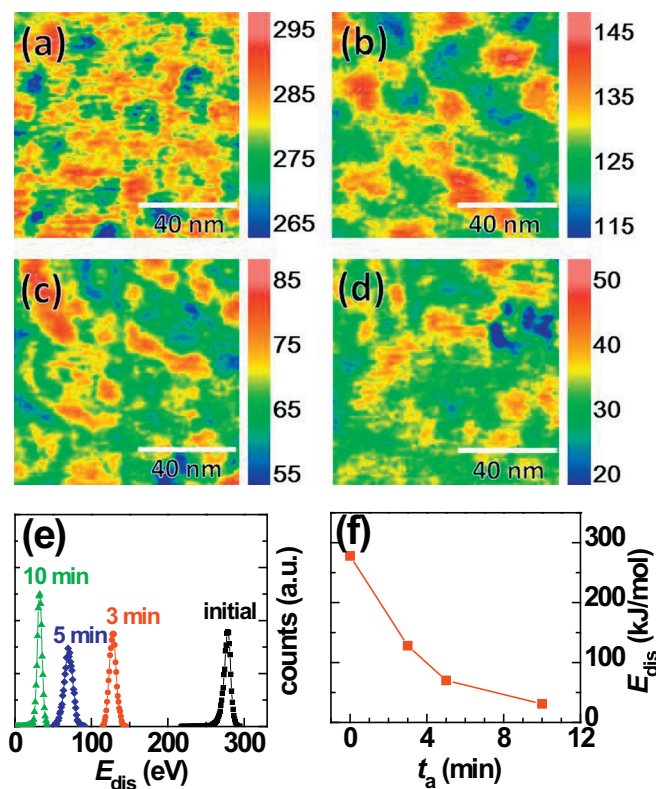
Fig. 5. The nanoscale viscoelastic heterogeneity for samples annealed at 733 K for different times (a) as-spun, (b) t_a = 3 min, (c) t_a = 5 min, (d) t_a = 10 min. The color bar represents E_{dis}, in unit of eV. (e) The statistical distribution of dissipation energy E_{dis} for as-spun and annealed samples. (f) The evolution of E_{dis} (peak value) along with annealing time t_a.

relaxation. During β relaxation, the magnetic properties are enhanced superbly without noticeable change of mechanical properties. During α relaxation, the magnetic properties don't change very much but the mechanical properties get deteriorated. The change of properties is found to be correlated with the evolution of viscoelastic microstructures. These results are helpful for designing optimum protocols for fabricating metallic glasses with both superior magnetic and mechanical properties by controlling the relaxation process.

Declaration of interest statement

We declare that all authors have no financial and personal relationships with other people or organizations that can inappropriately influence our work, there is no professional or other personal interest of any nature or kind in any product, service and/or company that could be construed as influencing the position presented in, or the review of, the manuscript entitled.

References

[1] D.C. Jiles, Acta Mater. 51 (2003) 5907.
[2] A. Inoue, F.L. Kong, Q.K. Man, B.L. Shen, R.W. Li, F. Al-Marzouki, J. Alloys Compd. 615 (2014) S2.
[3] H.R. Lashgari, D. Chu, Shishu Xie, Huande Sun, M. Ferry, S. Li, J. Non-Cryst. Solids 391 (2014) 61.
[4] A.D. Wang, C.L. Zhao, H. Men, A.N. He, C.T. Chang, X.M. Wang, R.W. Li, J. Alloys Compd. 630 (2015) 209.
[5] J.J. Lewandowski, W.H. Wang, A.L. Greer, Phil. Mag. Lett. 85 (2005) 77.
[6] M. Aljerf, K. Georgarakis, A.R. Yavari, Acta Mater. 59 (2011) 3817.
[7] X.F. Liang, A.N. He, A.D. Wang, J. Pang, C.J. Wang, C.T. Chang, K.Q. Qiu, X.M. Wang, C.T. Liu, J. Alloys Compd. 694 (2017) 1260.
[8] Y.Y. Zhao, A. Inoue, C.T. Chang, J. Liu, B.L. Shen, X.M. Wang, R.W. Li, Sci. Rep. 4 (2014) 5733.
[9] G. Kumar, P. Neibecker, Y.H. Liu, J. Schroers, Nat. Commun. 4 (2013) 1536.
[10] A. Ishii, F. Hori, A. Iwase, Y. Fukumoto, Y. Yokoyama, T.J. Konno, Mater. Trans. 49 (2008) 1975.
[11] P. Zhang, J.J. Maldonis, Z. Liu, J. Schroers, P.M. Voyles, Nat. Commun. 9 (2018) 1129.
[12] Y. Tong, J.C. Qiao, C. Zhang, J.M. Pelletier, Y. Yao, J. Non-Cryst. Solids 452 (2016) 57.
[13] B. Huang, Z.G. Zhu, T.P. Ge, H.Y. Bai, B.A. Sun, Y. Yang, C.T. Liu, W.H. Wang, Acta Mater. 110 (2016) 73.
[14] L.J. Song, W. Xu, J.T. Huo, J.Q. Wang, X.M. Wang, R.W. Li, Intermetallics 93 (2018) 101.
[15] P. Luo, P. Wen, H.Y. Bai, B. Ruta, W.H. Wang, Phys. Rev. Lett. 118 (2017) 225901.
[16] J.C. Qiao, Y.J. Wang, L.Z. Zhao, L.H. Dai, D. Crespo, J.M. Pelletier, L.M. Keer, Y. Yao, Phys. Rev. B 94 (2016) 104203.
[17] G. Ruocco, S. Capaccioli, Physics 10 (2017) 58.
[18] I. Gallino, D. Cangialosi, Z. Evenson, L. Schmitt, S. Hechler, M. Stolpe, B. Ruta, Acta Mater. 144 (2018) 400.
[19] V.A. Khonik, K. Kitagawa, H. Morii, J. Appl. Phys. 87 (2000) 8440.
[20] G. Ruitenberg, Thermochim. Acta 404 (2003) 207.
[21] H.B. Yu, W.H. Wang, H.Y. Bai, Y. Wu, M.W. Chen, Phys. Rev. B 81 (2010) 220201.
[22] W.H. Wang, Prog. Mater. Sci. 57 (2012) 487.
[23] Y.H. Liu, D. Wang, K. Nakajima, W. Zhang, A. Hirata, T. Nishi, A. Inoue, M.W. Chen, Phys. Rev. Lett. 106 (2011) 125504.
[24] H. Wagner, D. Bedorf, S. Kuchemann, M. Schwabe, B. Zhang, W. Arnold, K. Samwer, Nat. Mater. 10 (2011) 439.
[25] F. Zhu, H.K. Nguyen, S.X. Song, D.P.B. Aji, A. Hirata, H. Wang, K. Nakajima, M.W. Chen, Nat. Commun. 7 (2016) 11516.
[26] Y. Yang, J.F. Zeng, A. Volland, J.J. Blandin, S. Gravier, C.T. Liu, Acta Mater. 60 (2012) 5260.
[27] J.C. Ye, J. Lu, C.T. Liu, Q. Wang, Y. Yang, Nat. Mater. 9 (2010) 619.
[28] W. Jiao, P. Wen, H.L. Peng, H.Y. Bai, B.A. Sun, W.H. Wang, Appl. Phys. Lett. 102 (2013) 081904.
[29] S. Ouyang, L.J. Song, Y.H. Liu, J.T. Huo, J.Q. Wang, W. Xu, J.L. Li, C.T. Wang, X.M. Wang, R.W. Li, Phys. Rev. Mater. 2 (2018) 063601.
[30] Y.N. Chen, T. Egami, J. Appl. Phys. 50 (1979) 7615.